Øystein Godøy
Det norske meteorologiske institutt

# Precipitation estimation using satellite remote sensing

NOTAT
Nr. 13
1998

HYDRA

-ET FORSKNINGSPROGRAM OM FLOM


## HYDRA - et forskningsprogram om flom

HYDRA er et forskningsprogram om flom initiert av Norges vassdrags- og energiverk (NVE) i 1995. Programmet har en tidsramme på 3 år, med avslutning medio 1999, og en kostnadsramme på ca. 18 mill. kroner. HYDRA er i hovedsak finansiert av Olje- og energidepartementet.

Arbeidshypotesen til HYDRA er at summen av alle menneskelige påvirkninger i form av arealbruk, reguleringer, forbygningsarbeider m.m. kan ha økt risikoen for flom.

Målgruppen for HYDRA er statlige og kommunale myndigheter, forsikringsbransjen, utdannings- og forskningsinstitusjoner og andre institusjoner. Nedenfor gis en oversikt over fagfelt/tema som blir berørt i HYDRA:

- Naturgrunnlag og arealbruk
- Tettsteder
- Flomdemping, flomvern og flomhandtering
- Skaderisikoanalyse
- Miljøvirkninger av flom og flomforebyggende tiltak
- Databaser og GIS
- Modellutvikling

Sentrale aktører i HYDRA er; Det norske meteorologiske institutt (DNMI), Glommens og Laagens Brukseierforening (GLB), Jordforsk, Norges geologiske undersøkelse (NGU), Norges Landbrukshøgskole (NLH), Norges teknisk-naturvitenskapelige universitet (NTNU), Norges vassdrags- og energiverk (NVE), Norsk institutt for jord- og skogkartlegging (NIJOS), Norsk institutt for vannforskning (NIVA), SINTEF, Stiftelsen for Naturforskning og Kulturminneforskning (NINA/NIKU), Norsk Regnesentral (NR), Direktoratet for naturforvaltning (DN), Østlandsforskning (ØF) og universitetene i Oslo og Bergen.

## HYDRA - a research programme on floods

HYDRA is a research programme on floods initiated by the Norwegian Water Resources and Energy Administration (NVE) in 1995. The programme has a time frame of 3 years, terminating in 1999, and with an economic framework of NOK 18 million. HYDRA is largely financed by the Ministry of Petroleum and Energy.

The working hypotesis for HYDRA is that the sum of all human impacts in the form of land use, regulation, flood protection etc., can have increased the risk of floods.

HYDRA is aimed at state and municipal authorities, insurance companies, educational and research institutions, and other organization.

An overview of the scientific content in HYDRA is:

- Natural resources and land use
- Urban areas
- Databases and GIS
- Risk analysis
- Flood reduction, flood protection and flood management
- Environmental consequences of floods and flood prevention measures
- Modelling

Central institutions in the HYDRA programme are; The Norwegian Meteorological Institute (DNMI), The Glommens and Laagens Water Management Association (GLB), Centre of Soil and Environmental Research (Jordforsk), The Norwegian Geological Survey (NGU), The Agriculture University of Norway (NLH), The Norwegian University of Science and Technology (NTNU), The Norwegian Water and Energy Administration (NVE), The Norwegian Institute of Land Inventory (NIJOS), The Norwegian Institute for Water Research (NIVA), The Foundation for Scientific and Industrial Research at the Norwegian Institute of Technology (SINTEF), The Norwegian Institute for Nature and Cultural Heritage Research (NINA/NIKU), Norwegian Computing Center (NR), Directorate for Nature Management (DN), Eastern Norway Research Institute (ØF) and the Universities of Oslo and Bergen.

# Contents

CHAPTER 1

# Introduction

## 1.1 Background

Estimates of the precipitation in an geographical area are used in hydrological models operated by the Norwegian Water Resources and Energy Administration (NVE). At present this information is collected from DNMIs weather observing stations at ground. However, other data sources, e.g. remote sensing techniques, exist. This report address the use of data from operational meteorological satellites. The possibility of using weather radar for this purpose in Norway is briefly discussed.

The operational weather satellites in the NOAA[1]- POES[2]- program (currently NOAA-12 and NOAA-14) has relatively high temporal resolution in the Nordic area (10-15 passages a day in the area of interest of DNMI) and should be well suited for this purpose.

Weather radar is another observing tool that is well suited for collecting information about the spatial distribution of precipitation. At present DNMI operates only one weather radar. A new radar will be operational from mid 1999. Together with the present radar, this will cover a large part of southern Norway, including test areas defined later in this report. Further extension of the radar network is planned. Weather radar data is only briefly discussed in this report, no example of use is included. However, it may be a useful source of data in the future, both on its own and in combination with satellite information.

## 1.2 Objective

The primary objective of this work is to gain an improved estimate of the spatial variability of precipitation in flooding situations by the use of remotely sensed data.

## 1.3 Method

The local distribution of precipitation is estimated by the use of remotely sensed data for some chosen precipitation fields and situations. In cooperation with NVE, the potential positive effect of using these data instead of the smoothed data from the operational models is examined.

This report describes different methods and satellite systems that may be used for estimates of precipitation, but testing of algorithms are only performed using NOAA AVHRR data collected from the operational NOAA POES program. More information about the actual testing of algorithm and areas being studied is given in CHAPTER 4.

1. National Oceanic and Atmospheric Agency
2. Polar Orbiting Environmental Satellites

## 1.4 Structure of the report

The report first give a brief introduction to the most common methods used in order to estimate precipitation using remotely sensed data. Then a brief introduction to the available data at DNMI is given before an experiment using an algorithm implemented at DNMI is performed over an area including some of the area defined by NVE.

CHAPTER 2

# Estimates of precipitation using remotely sensed data

## 2.1 Introduction

The main problem using satellite data from the operational meteorological satellites (METEOSAT and NOAA) to estimate precipitation is that the instruments carried by these satellites are mainly designed to observe clouds. Not all clouds produce precipitation.

The techniques used to estimate precipitation can be divided in three categories (Kidder and Vonder Haar, 1995). Techniques that use visible and/or infrared data, techniques that use passive microwave data and finally techniques that use active microwave data (radar). In addition to Kidder and Vonder Haar (1995), Petty (1995) also has given a review of the current techniques for precipitation estimations using satellite remote sensing data.

## 2.2 Visible and infrared techniques

These techniques estimate the precipitation from a cloud based on the radiation observed above the cloud. Thus these techniques are indirect as the precipitation (raindrops) itself is not observed.

Barrett and Martin (1981) divided these techniques in four main categories; Cloud indexing, Bi-spectral techniques, Life-History techniques and Cloud-Model techniques. All techniques are further described in Kidder and Vonder Haar, 1995 with examples of implementations. Only a brief overview is given here.

The electromagnetic radiation denoted as visible (shortwave) is usually in the range of 0.3-4 μm and the infrared (longwave) radiation is in the range of 4-100 μm [1].

These wavelengths are observed by several meteorological satellites. The Advanced Very High Resolution Radiometer (AVHRR) which is currently flown on the NOAA-12 and NOAA-14 has 5 channels observing this radiation (AVHRR/2). NOAA-15 which was launched 13 May 1998 carries a newer version (AVHRR/3) of the AVHRR instrument and observes in 6 spectral intervals. The characteristics of the current and future versions of the AVHRR instrument is given in TABLE I.

1. No general definition is given, it is usually left to the author (see Tipler 1982).

**TABLE I AVHRR characteristics.**

| Parameter | AVHRR/2 | AVHRR/3 |
|---|---|---|
| Ground Resolution | | |
| Nadir | 1.1 km | 1.1 km |
| End of scan | 2.3·6.4 km | 2.3·6.4 km |
| Scan Line | | |
| Angle from nadir | ±55.3° | ±55.3° |
| Distance from nadir | ±1500 km | ±1500 km |
| Steps | 2048 | 2048 |
| Channels (half-power points) | | |
| 1 | 0.55-0.68 μm | 0.55-0.68 μm |
| 2 | 0.725-1.10 μm | 0.725-1.10 μm |
| 3 | 3.55-3.93 μm | A: 1.56-1.66 μm |
| | | B: 3.55-3.93 μm |
| 4 | 10.3-11.3 μm | 10.3-11.3 μm |
| 5 | 11.5-12.5 μm | 11.5-12.5 μm |

The AVHRR instrument is among the most successful instruments ever carried by a meteorological satellite. It has been operated for 20 years and will be operating for another 20 years as the new generation of NOAA POES (NOAA-15, etc.), the EUMETSAT Polar System (METOP) and the next generation of geostationary satellites operated by EUMETSAT (METEOSAT Second Generation - MSG) respectively will carry a similar and modified version of the instrument. The MSG programme will have an instrument sampling at 0.6, 0.8, 1.6, 3.8, 6.2, 7.3, 8.7, 9.7, 10.8, 12.0, 13.4 μm and the nadir ground resolution will be 1 and 3 km (VIS) and 3 km (IR).

### 2.2.1 Cloud indexing

This techniques assigns a rain rate to every cloud type identified. The rain rate in an area is found by:

$$R = \sum_i r_i f_i \qquad \text{EQ. 1}$$

where $r_i$ is the rain rate assigned to cloud type $i$ and $f_i$ is the fraction of time the area is covered by cloud $i$. Thus technique is closely related to à cloud classification scheme. Examples of this approach is found in Follandsbee (1973), Wu et al. (1985) and Arkin and Meisner (1987).

This is the oldest method, but it is still useful.

### 2.2.2 Bi-spectral techniques

The principle of these techniques are based on the assumption that most precipitating clouds are optically thick.

The higher reflectance in the visible (can be related to optical thickness) and colder cloud tops (can be related to vertical extension of cloud), the more precipitation is expected from the cloud. However, this simple assumption fails for several cloud types. Stratus clouds reflect well, but do not precipitate much, cirrus clouds are cold, but do not precip-

itate much. This knowledge is used to expect less precipitation from cold, but dark clouds (thin cirrus) and bright, but warm clouds (stratus).

Despite these problems, bi-spectral techniques is used in the majority of the published techniques for satellite rainfall estimation. In this study, bi-spectral techniques also includes the pure IR techniques which is a necessary alternative to the bi-spectral techniques at high latitudes since no or little reflected solar light is available much of the year.

The pure IR techniques can be used when no reflected solar light is available e.g. during tropical night or polar winter. It is much used in tropical regions and relies on empirical relationships between e.g. the monthly mean outgoing longwave radiation and an area averaged rainfall (e.g. Arkin, 1984).

A technique relying on the bi-spectral techniques for precipitation estimation is the RAINSAT system (Lovejoy and Austin, 1979, Bellon et al., 1980, Bellon et al., 1992). In the latest version of this system, weather radar data is integrated with a pure bi-spectral technique. This system has been in operational use both in Canada and Spain for some years.

### 2.2.3 Life-History techniques

These techniques is based on the fact that the rain rate of clouds, and in particular of the convective clouds, is a function of the development of the cloud. They relate the area of the cloud to the development of the cloud system, thereby connecting a rain rate to the cloud. Some examples of life-history algorithms are given by Griffith et al. (1978) and Scofield (1987). The first one is fully automated, while the other require some human interaction. The method of Scofield (1987) was classified as a life-history method by Barrett and Martin (1981), but Kidder and Vonder Haar (1995) defines it as a cloud model technique as it is based on a conceptual cloud model.

Negri et al (1984) removed the time-history from the method of Griffith et al. (1978) and gained a results that were comparable in quality to the original technique. This suggesting that the time-history information contributes little to better accuracy in the estimates. In essence the method of Negri et al. (1984) is a bi-spectral technique which attributes rain rates within the cloud according to the cloud top temperature.

### 2.2.4 Cloud Model techniques

In order to improve the techniques used to estimate precipitation from visible and infrared satellite data, Kidder and Vonder Haar (1995) believes it is important to improve the description of cloud physics. They refer to several attempts using cloud models in this process.

Examples of this technique can be found in Wylie (1979), Adler and Negri (1984), and Scofield and Oliver (1977).

Wylie (1979) used a one-dimensional cloud model to adjust the precipitation estimates as these usually are site dependent. A more complex use of a one-dimensional model was performed by Adler and Negri (1984) who used the cloud model to find a relationship between cloud top temperature, rain rate and raining area. This relationship is tabulated and used as a lookup table where analysed for cloud top temperatures from the IR imagery are used as index. A rain rate and raining area are assigned for each pixel. The Scofield and Oliver (1977) technique is operationally used by NOAA NESDIS and includes a conceptual cloud model, but is not an automated technique. A trained satellite

meteorologist locates spectral signatures associated with precipitation in satellite imagery. For assignment of a rain rate to each pixel a decision tree is used (reproduced in Kidder and Vonder Haar, 1995, pp.332-333).

### 2.2.5 Summary on visible and infrared techniques

It is difficult to estimate the precipitation with sufficient accuracy using visible and infrared techniques because these measurements are sensitive to the integrated water and ice content of the clouds. Emitted and scattered radiation from cloud droplets and ice crystals dominate over the contribution from precipitation particles. That is, the relative contribution of the upper part of the cloud to the satellite observed radiation is larger than from the lower part where most of the precipitation forms. Evaporation and collision-coalescence below the cloud base can reduce the correlation between precipitation reaching the ground and spectral signatures in the visible and infrared further.

The reliable precipitation product obtainable from visible and infrared techniques are qualitative estimates like light, moderate and heavy. In order to improve these methods, combination with other data sources like microwave or surface observations are required. Given a surface observation this may be used to assign precipitation rates to different spectral signatures defined in a precipitation analysis scheme. This may also be used to continuously update threshold values in such an analysis scheme.

## 2.3 Passive microwave

Remotely sensed observations in the microwave region of the electromagnetic spectrum has proven to be useful for estimates of precipitation amounts. Contrary to the visible and infrared techniques, observations in the microwave region of the electromagnetic spectrum respond physically to the precipitation or ice particles within the clouds. The disadvantage of techniques using passive microwave radiation to estimate precipitation is that the sensors have poor temporal and spatial resolution.

Three wavelengths (approximately: 18 GHz$\leftrightarrow$1.7 cm, 37 GHz$\leftrightarrow$0.81 cm, 85 GHz$\leftrightarrow$0.35 cm) have mainly been used for observations of the precipitation with passive sensors. The absorption and scattering properties of these wavelengths were examined by Spencer et al. (1989). They found that:

- Ice mainly scatters microwave radiation.
- Liquid drops both absorbs and scatter, but absorption dominates.
- Absorption and scattering increase with frequency and rain rate.

The results of Spencer et al. (1989) indicates that the microwave spectrum can be divided in roughly three parts. Below approximately 22 GHz (~1.36 cm) absorption dominates the atmospheric transfer of microwave radiation. Between 22 GHz and approximately 60 GHz (~0.5 cm) absorption and scattering are of equal importance, but at frequencies higher than this scattering dominates.

The phase of the precipitation also affects the observed signal. Below 20 GHz ice is practically transparent, while it dominates above 60 GHz.

Passive microwave instruments are carried by the polar orbiting Defence Meteorological Satellite Programme (DMSP). Especially the Special Sensor Microwave Imager (SSM/I) has proven useful in precipitation estimation. This instrument observes at 19.35, 22.235, 37.0 and 85.5 GHz. The footprint of the instrument changes with channel, ranging from 13 $\times$ 15 km (85.5 GHz) to 43 $\times$ 69 km (19.35 GHz).

Methods using measurements of microwave radiation to estimate precipitation may be divided in two main categories: attenuation and scattering methods.

### 2.3.1 Attenuation methods

Attenuation based methods utilize the absorption and emission effects caused by liquid precipitation.

Petty (1990) describes such a method utilizing the reduction of polarization of ocean surface emitted radiation by precipitating clouds. The reduction is described by the normalized polarisation difference in the SSM/I 37 GHz channel ($P_{37}$).

$$P_{37} = (T_{37V} - T_{37H})\exp(0.0151U + 0.00607V - 4.40) \quad \text{EQ. 2}$$

where $T$ is the (respectively vertical and horizontally polarised) brightness temperatures, $U$ the near-surface wind speed and $V$ the integrated water vapour. The last two may be collected from NWP[1] models or observations. Precipitation areas are located using the relations in TABLE II.

**TABLE II Relation between the normalized polarization difference in the SSM/I 37 GHz band and precipitation (Petty, 1990, Karlsson, 1997).**

| LT[a] | $P_{37}$[b] | UT[c] | Description |
|---|---|---|---|
| | $P_{37} <$ | 0.8 | Precipitation will ordinarily occur |
| 0.8 | $< P_{37} <$ | 0.9 | at most light precipitation |
| 0.9 | $< P_{37}$ | | precipitation is unlikely to occur |

a. Lower threshold.
b. Normalized polarization difference in the SSM/I 37 GHz band.
c. Upper threshold.

The definition of $P_{37}$ this way compensates for the dependence of the surface wind stress of the ocean, but a substantial amount of the attenuation is caused by large cloud droplets and not precipitation drops, limiting the possibility to estimate precipitation rates (Petty, 1990).

This is only one example of such a method, several others exist, but this one is much referenced in literature.

### 2.3.2 Scattering methods

A scattering based method was also described by Petty (1990). This use the SSM/I 85 GHz channel and the relation:

$$S_{85}(K) = P_{85}T_{85V0} + (1 - P_{85})T_C - T_{85V} \quad \text{EQ. 3}$$

where $S_{85}$ is the polarisation corrected brightness temperature depression (scattering index), $T_{85V0}$ is vertically polarised brightness temperature of 85 GHz under cloudfree conditions, $T_C$ is the limiting brightness temperature of an increasingly opaque non-scattering cloud layer (typically 273 K) and $P_{85}$ is the 85 GHz equivalent of EQ. 2 (constants are tuned). $S_{85}$ was found to be larger than 10 K for precipitating clouds. Larger values may be used to infer precipitation rates.

1. Numerical Weather Prediction

This is only one example of such a method, several others exist, but this one is much referenced in literature.

### 2.3.3 Summary on passive microwave techniques

Passive microwave data like the SSM/I are more suitable for precipitation estimates over ocean areas than land areas as polarisation effects are more uniform over water. Drawbacks of these data are the large footprint of the sensors and the narrow ground swath. At the SSM/I instrument the footprint depends on the spectral interval used. The 85 GHz footprint is the smallest at $13 \times 15$km.

## 2.4 Active microwave (Weather Radar)

Weather radars have been operated on the earths surface for several years. They are active instruments that operate in the microwave portion of the electromagnetic spectrum. The radar sends out a pulse and observes the frequency, phase and power of the returned signal. Three main types of weather radars are commonly used. These are X-, C- and S-band radars. Originally the X-band (3 cm$\leftrightarrow$10 GHz) radar was used as this is quite cheap and has a moderate size antenna. However, this wavelength is exposed to atmospheric attenuation so the S-band (10 cm$\leftrightarrow$3 GHz) radar was developed. This is less exposed to attenuation, but requires a larger antenna and is more expensive. The current mostly used compromise is the C-band radar (5 cm$\leftrightarrow$6 GHz).

Several objects can return the emitted signal, but at the wavelengths usually chosen for weather radars, precipitation is the major echo source. However, other objects like birds, dust and insects may give echoes as well. A major problem using a ground based weather radar is ground clutter due to echoes from buildings and topographic features. This may be filtered away, but there is always a risk of filtering too much data away, also removing the interesting signal. Filtering of ground clutter is specific for each radar site. The received signal has to be related to the geophysical parameter interesting to the user. Usually this is precipitation. In order to do this a relationship is established between the received echo and the precipitation rate. Usually this is done by an empirical model based on a chosen droplet size distribution believed to be representative for the area, type of precipitation and season. However, large differences in these relations are found as a function of cloud particle phase (ice or water), cloud type (droplet distributions vary much between cloud types) and season (cloud types vary through the season as the atmosphere changes, also a consequence of the cloud type and phase). Thus in order to use a weather radar for estimates of the precipitation amount an extensive program of calibration against ground measurements is required. It may however, easy provide the user with a qualitative impression of the precipitation in an area.

Some people has dreamed of placing a weather radar on a satellite. This would give better spatial coverage and thus improve the data of precipitating areas. However, several problems are connected to this task. For example, the radar is an active system that requires a lot of power to transmit a pulse. The present satellite instruments require an order of magnitude less power (Kidder and Vonder Haar, 1995). Furthermore, the satellite moves quite fast over the underlying surface. Radar measurements usually requires several observations of the same atmospheric volume for accurate estimates to be made. This is complicated on a flying platform which also will cause the antenna to be looking in different directions as the signal is emitted and when the returned signal is received. Several other problems are found as well, some of them are described at pages 349 and 350 in Kidder and Vonder Haar (1995).

Despite all these problems a satellite borne radar was launched in the Tropical Rainfall Measuring Mission. This is a NASA[1] / NASDA[2] mission which is designed to measure tropical rainfall and its diurnal variability in grid boxes of $10^5$ km$^2$ on a monthly time scale. The precipitation observing radar is operating on 13.8 GHz (~2.17 cm) with a 4.3 km$^2$ IFOV at a 220 km wide swath. This satellite borne radar was launched on November 27, 1997 and is now operating, but does not provide information at high latitudes as the inclination is 35° to Equator (see Kidder and Vonder Haar, 1995, chapter 2.4 for more on satellite orbits).

## 2.5 Summary

Visible and infrared techniques using data from the operational meteorological satellites is useful for qualitative estimates of the precipitation. These techniques are well suited for detection of potential precipitation maxima and minima at high temporal and spatial resolution. In order to achieve quantitative estimates of the precipitation intensity observations in the microwave part of the electromagnetic spectrum is required. This can be either active or passive observations performed by a satellite carried or ground based instrument. The satellite borne microwave instruments have usually poorer spatial resolution than visible and infrared instruments.

The passive microwave instruments are best suited for precipitation estimates over ocean areas as the background polarisation factor is more uniform there.

Weather radars are well suited for precipitation estimates over land.

1. National Aeronautics and Space Administration (US).
2. National Space Development Agency (Japan).

CHAPTER 3

# Estimation of precipitation using remotely sensed data at DNMI

## 3.1 Introduction

DNMI operates a receiving station for both NOAA/AVHRR and METEOSAT/MVIRI data at Blindern, Oslo. MVIRI data is received every 30 minutes while AVHRR data covering the area of interest are received 10-15 times a day. Information from the single weather radar operated by DNMI at present is available every 15 minutes covering south-eastern Norway. A new radar in southern Norway will be operational from the summer of 1999. SSM/I data is currently not received through operational lines at DNMI, but actions has been taken to receive these data through GTS from UK Met. Office in Bracknell (UK).

The research and development of methods for precipitation estimation using remotely sensed data at DNMI has been focused at NOAA/AVHRR data. These data are suitable only for qualitative estimates of the precipitation (see CHAPTER 2).

## 3.2 Satellite imagery analysis

In the focal area of DNMI, data from the polar orbiting NOAA satellites are most interesting, both for subjective and objective interpretation of the data. The geostationary METEOSAT/MVIRI data is not useful for objective interpretation at these latitudes as the large viewing angle creates a very large footprint and atmospheric effects complicates the analysis.

An Automatic Interpretation of Remote sensing data (AIR), essentially an objective classification (analysis) system for NOAA/AVHRR data (Godøy and Sunde, 1996), is developed at DNMI. The main purpose of AIR is to analyse the available remote sensing data, not to produce a forecast. Some effort has however been provided to establish linear extrapolation routines for short range forecasts (0-3 hours) using cross-correlation techniques and wind fields from the numerical models. In the present version of AIR, AVHRR data is combined with NWP data from the operational HIRLAM model at DNMI. This is a threshold or box classification algorithm.

Two algorithms are developed, one for day-time imagery and one for night-time, the difference being the availability of reflected solar light for the algorithm. The system is described in Godøy and Sunde (1996), Breivik et al. (1997) and Godøy (1997). A short review is given here.

The present classification use AVHRR channels 1, 2, 3, 4, 5, and HIRLAM NWP output during day-time and AVHRR channels 3, 4, 5, and NWP output during night-time. A Terrain Elevation Database (TED, Godøy, 1997) covering Norway is used to adjust NWP surface temperatures for terrain and a land-sea mask covering Europe and Greenland/ Svalbard is used where TED is not available.

During day-time, AVHRR channels 1 (0.6 μm) and 2 (0.9 μm) are adjusted for the solar zenith angle.

The classes available during day- and night-time is presented in TABLE III.

**TABLE III Classes used in the AVHRR classification system implemented at DNMI.**

| Day-time | Night-time |
|---|---|
| cloudfree | cloudfree |
| snow or ice | N/A[a.] |
| Risk of fog or low stratus | Risk of fog or low stratus |
| Light precipitation[b.] | Light precipitation |
| Heavy precipitation[b.] | Heavy precipitation |
| Risk of deep convection | N/A[a.] |
| Low level clouds | Low level clouds |
| Medium level clouds | Medium level clouds |
| High level clouds | High level clouds |

a. Not Available

b. During day time a specific precipitation analysis may be performed giving 4 different classes (risk of, light, moderate and heavy precipitation). The heavy precipitation class then includes many of the pixels that else would be classed as risk of deep convection.

As indicated in a footnote of TABLE III the precipitation analysis is slightly modified to that presented in Godøy and Sunde (1996). The main difference is that more classes are used during day time when the classification system is operated in a precipitation analysis mode. It is results from the precipitation analysis during day time that is presented in this report.

Basically the present configuration is a simple bi-spectral technique using both visible and infrared information when visible is available and only infrared radiation at other times. The NWP data is used to help the classification. There is no need for human intervention by typing threshold values etc., and NWP data is at no point allowed to overrule the satellite data. At present temperature threshold values are collected from HIRLAM and the cloud top temperatures computed from satellite data are compared with these. The temperature information might just as well be collected from observational temperature profiles, though the software system does not support this yet. Threshold values for the reflected solar radiation is static at present, but plans are made towards combined use of databases and radiative transfer models in the future.

The precipitation analysis is based on the assumption that the brighter and colder cloud tops, the higher risk of precipitation. This type of precipitation analysis using visible and infrared radiances has been performed operationally in the RAINSAT (Bellon et al., 1980) and SCANDIA (Karlsson, 1997) systems. In RAINSAT weather radar data were used as well, but SCANDIA is only using satellite and NWP data. The system implemented at DNMI is quite similar to the precipitation analysis in SCANDIA. TABLE IV gives an overview of the features (both spectral and auxiliary) used to perform the precipitation analysis.

**TABLE IV Spectral and auxiliary features used in the precipitation analysis based upon NOAA AVHRR data and NWP data from HIRLAM.**

| Acronym | Quantity | Description |
|---|---|---|
| A1 | Albedo[a.] | Bright clouds (high A1) usually, but not always, have high risk of precipitation. |
| T4 | Brightness temperature (K[b.]) | Cold clouds usually, but not always, have high risk of precipitation. |
| T3-T4 | Difference in brightness temperature (K) | This feature is used to identify Cb[c.] as these clouds have high risk of precipitation. |
| T4-T5 | Difference in brightness temperature (K) | This feature is used to prevent thin and cold ice clouds from being labelled as precipitation clouds. |
| T700 | Temperature (K) | 700 hPa temperature from HIRLAM, continuously updated. |
| T500 | Temperature (K) | 500 hPa temperature from HIRLAM, continuously updated. |

a. A more correct term would be bi-directional reflectance.
b. Kelvin
c. Cumulonimbus

A schematic presentation of the basic principles of the precipitation analysis is presented in FIGURE 1 (redrawn from Karlsson, 1997). In FIGURE 1 only the first two features of TABLE IV is presented directly, but the threshold values for the brightness temperature of channel 4 is estimated on the basis of the 500 and 700 hPa temperatures collected from HIRLAM. The spectral feature of precipitating clouds are indicated by shading. In the precipitation analysis implemented at DNMI, the remaining features of TABLE IV are used as well. How the different features are used are discussed below.

The A1 feature is only used when the solar elevation is above 20°. It is at present a static parameter, which however may be changed during the year and geographical region examined. The present threshold for precipitation is 40%, slightly lower than indicated by FIGURE 1 as more clouds than indicated in this figure may give precipitation. Higher values are related to heavier precipitation as indicated in FIGURE 1.

T4 is used with dynamic threshold values. It can be used both day and night, a useful property at the high latitudes of Norway. Dynamic threshold values are collected from HIRLAM (500 and 700 hPa temperature fields). Colder cloud tops are related to heavier precipitation as indicated in FIGURE 1.

The T3-T4 spectral feature is used for detection of Cumulonimbus clouds, convective clouds with a large vertical extent that may give substantial precipitation amounts in a short time interval. These clouds reflect well in AVHRR channel 3 (Liljas, 1986, Setvak and Doswell, 1991). In the present version of the precipitation analysis values of T3-T4 larger than 17 K are used to identify the heavy precipitating Cumulonimbus during day time. At night the value in this feature is usually negative for Cumulonimbus clouds.

T4-T5 is usually less than 2.5 K and larger than -0.5 K (at large viewing angles, less at nadir[1.]) for optically thick clouds while thin Cirrus show differences outside this interval as AVHRR channel 5 is more sensitive to water vapour than channel 4.

1. Subsatellite point.

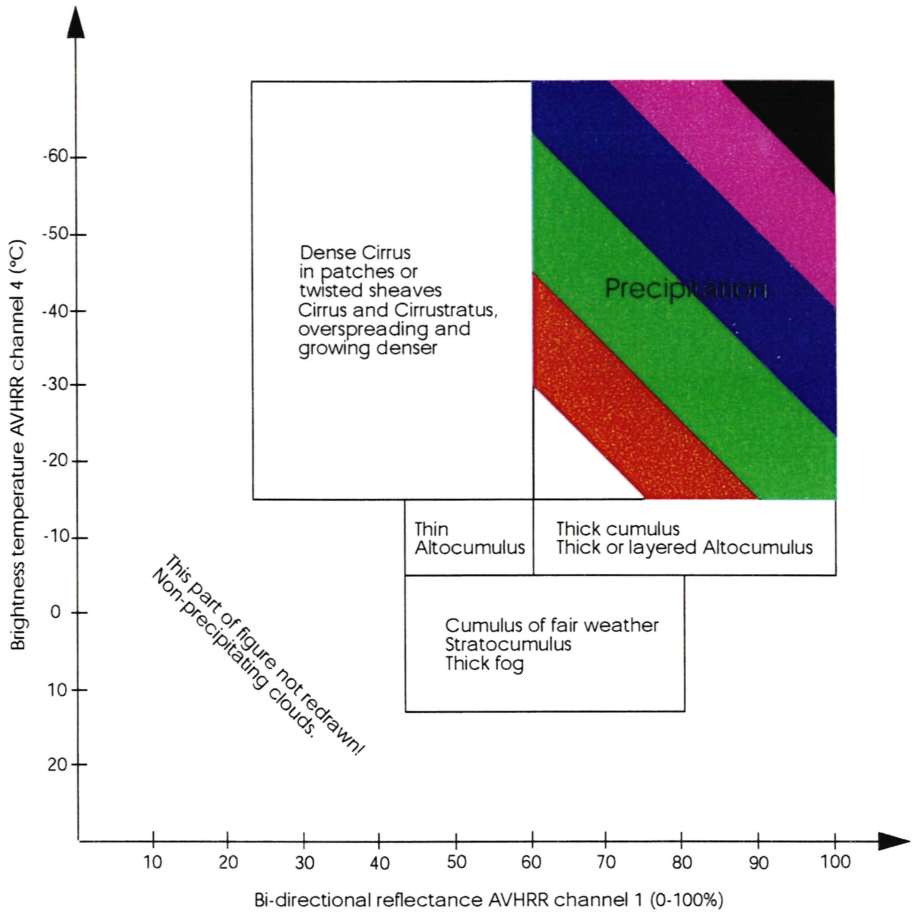


**FIGURE 1**

*Schematic description of the basic algorithm used for precipitation analysis. Other features are used as well in the scheme implemented, but these are of less importance and are mainly used to get a less "noisy" analysis. This figure is redrawn from Karlsson (1997) (Not the full figure as presented in Karlsson, 1997). The shaded area represents precipitating clouds and the degree of shading represents the precipitation intensity.*

The present version of the precipitation analysis (flowchart presented in FIGURE 2) is based upon threshold values collected from HIRLAM and literature (e.g. Karlsson, 1997). The schematic skewness of the precipitation intensity boxes in FIGURE 1 is not reproduced by the present algorithm.

In order to gain more knowledge of how the spectral features utilized in the system behave over Norway a database system for automatic training of the classification has been established. The training system will also be modified to include a feedback mechanism to the classification system but this is yet not implemented. This training system (Godøy, 1998), SAtellite and Ground OBservations (SAGOB), combines satellite and synoptic measurements. At present this system is only implemented for examination of the spectral signatures connected with fog, clear and snow covered conditions, but it will be extended to precipitation cases in near future.

So far AIR has been operated on radiometrically reduced resolution data (8-bit) without access to the information of the satellite zenith angle. A new processing chain which includes the satellite zenith angle in a radiometric full resolution product was implemented in December 1997.

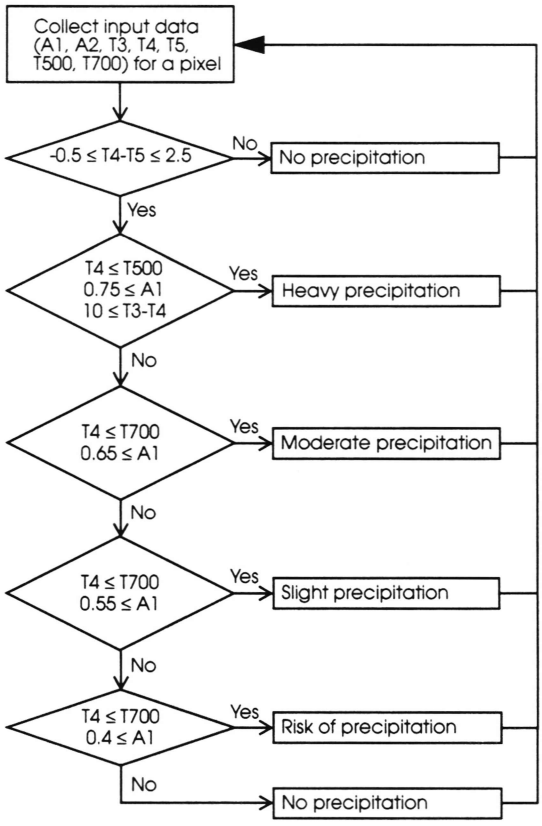


During night time the precipitation analysis use T4 and T4-T5 and the additional requirement that precipitating clouds has T5 ≥ T3-T4 to avoid cirrus clouds being labelled as precipitating clouds.

**FIGURE 2**

*Flowchart of the day time precipitation analysis scheme used at DNMI. All temperatures are given in Kelvin and bi-directional reflectances in values between 0 and 1 corresponding to 0-100%.*

## 3.3 Weather radar

At present DNMI operates one weather radar which was put into operation on April 1, 1988. This is an Ericsson Doppler[1] radar (C-band, 5 cm, ~6 GHz), and is situated in Asker (Hagahogget) near Oslo. It operates on a VAX/VMS platform with a display available to the operational forecaster at Blindern. In Doppler mode, the range covered by the radar is approximately 120 km (radius) and in conventional mode 240 km.

At present only pseudo CAPPI[2] products are available for the UNIX platform. A new weather radar with improved hardware and software will be operational from the summer of 1999. It will be situated at Hægebostad in Agder. Data from this will be better suited for use in the future remote sensing precipitation analysis scheme. It is assumed that the new radar will operate on a UNIX platform and that a 3D integrated precipitation product will be available for use in objective techniques. Collection of additional products from the old radar has also started.

1. In Doppler mode the Doppler shift of the radar signal is used to estimate the azimuth speed of the water particles reflecting the radar signal.
2. Constant Altitude Plan Position Indicator. A Plan Position Indicator product is transformed from polar coordinates to a Cartesian coordinate system.

However, in order to make full use of the weather radar data in a precipitation analysis scheme for quantitative precipitation estimates, careful calibration of the reflectivity against rain gauges is required. Thus, extensive development work is needed before weather radar data is fully implemented in the precipitation analysis described above.

Approximate positions and maximum coverage (in normal mode) of the present and planned radar are indicated in FIGURE 3. Ground clutter will affect the area covered effectively by the radar and at distances far from the radar lower levels of the atmosphere are not covered. Precipitation processes in those layers are not well discovered by the radar, however different techniques may be tested to improve precipitation estimation in these areas.

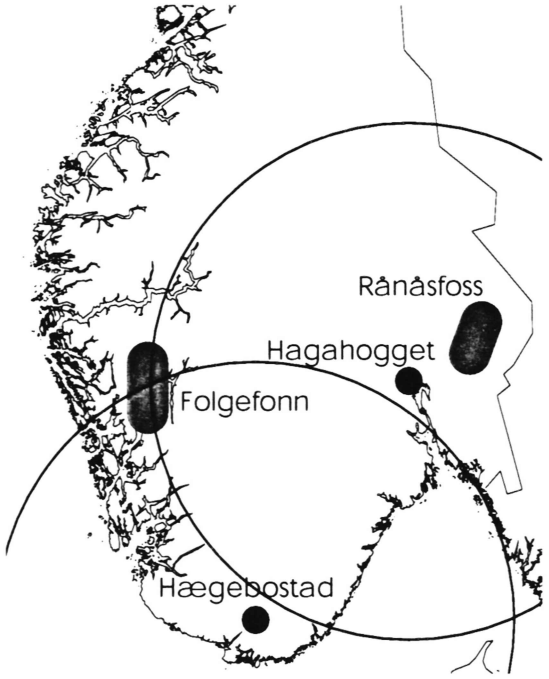


**FIGURE 3**

*Expected maximum radar coverage in normal mode and approximate positions of the present and planned DNMI radars by mid 1999.*

CHAPTER 4

# Experiments with the DNMI scheme on the areas selected by NVE

## 4.1 Introduction

Two areas has been chosen by NVE for validation of this project. In this chapter, experiments with the remote sensing precipitation scheme (AVHRR) at DNMI are described.

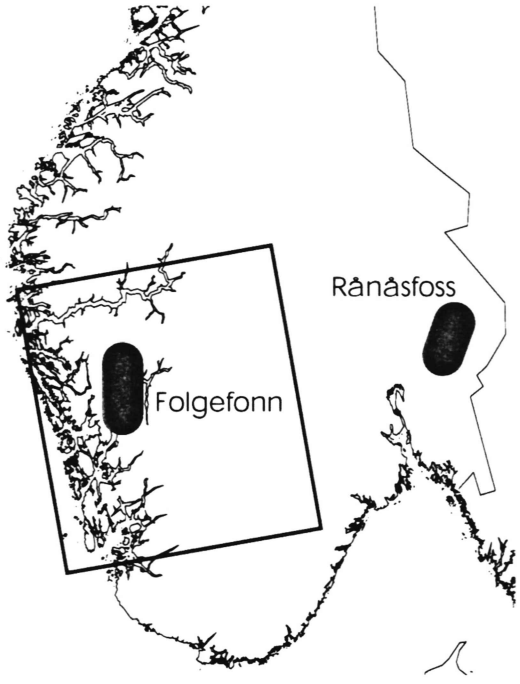


FIGURE 4

*The test areas defined by NVE. Rånåsfoss is placed in the south-eastern part of Norway, close to the border of Sweden. Folgefonn is placed in the western part of southern Norway, close to the Hardangerfjord and the glacier Folgefonni. The area studied here is indicated by the square box.*

The areas described in FIGURE 4 were selected by NVE for the project. This project has chosen a slightly larger area for validation of the estimates on spatial distribution of precipitation. The main reason for this is that in the present validation, only a short time period is examined, and in order to get a sufficiently large validation data set, an increased area with more synoptic stations was selected. The test area used here covers the southwestern part of Norway, including only the Folgefonn area defined above.

This report addresses validation of the day time precipitation analysis scheme. The precipitation analysis does, as indicated in CHAPTER 3, not give quantitative estimates, but qualitative estimate of the spatial distribution of precipitation.

## 4.2 Data

Testing of the precipitation analysis on real data is performed using 8-bit (reduced resolution) data which are calibrated and transformed to a Polar Stereographic map projection correct at 60°N and not rotated compared to the Greenwich meridian. The product area covering southern Norway in 1.5 km pixel resolution is chosen for the test. As only the day time algorithm is tested, data close to 12:00 UTC is chosen for better access to synoptic observations and reduction of anisotropic effects due to variable sun height.

NWP data are collected from the operational HIRLAM model at DNMI. The NWP model field closest in time is chosen.

The time period examined was 6-13 August 1998. Every day the NOAA-14 passage closest to 12:00 UTC was analysed. 12:00 UTC was chosen as many synoptic stations report at this hour ensuring a large number of precipitation observations.

## 4.3 Validation method

Validation of the precipitation analysis is performed using a method described by Inoue (1987) and Jackson et al. (1995) as well as more qualitative validation. The quantitative validation described below is only used for the detection of precipitation areas, not for the amount of precipitation as too few cases are studied.

Precipitation areas are validated against synoptic observations in the area. If a station has observed precipitation, and the precipitation analysis identifies at least one of the pixels in a 11×11 box (approximately 16.5×16.5 km) surrounding the station (FIGURE 5) as precipitating, the analysis is supposed to be correct. This large area is used to account for the maximum possible error in positioning the pixels. This is usually only relevant if TBUS[1] messages has not been updated for a long time. Furthermore, the area corresponds to the area usually viewed by an observer at the surface (Karlsson, 1993). According to Karlsson (1993), an observer on the ground usually sees low clouds in a radius of approximately 15km of the station, medium level clouds within 20km and high clouds within 30km of the station. Here an area relevant for low clouds are chosen. Another constraint in the analysis is that the maximum time offset between satellite image and synoptic observations should be less than 0.5 hours.

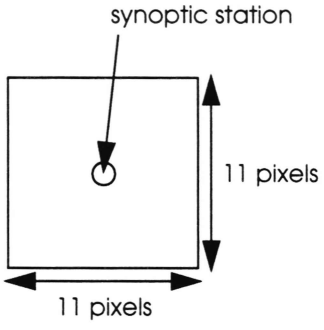


**FIGURE 5** *Search box for satellite data surrounding a synoptic station.*

The following variables:

*Sn*: number of pixels correctly classified as non precipitating
*Sr*: number of pixels incorrectly classified as non precipitating

1. Bulletins containing the information needed to position the satellite.

*Rn*: number of pixels incorrectly classified as precipitating
*Rr*: number of pixels correctly classified as precipitating

are used to estimate the Probability of Detection (*POD*) and the False Alarm Rate (*FAR*).

$$POD = \frac{Rr}{Rr + Sr} \quad \text{EQ. 4}$$

$$FAR = \frac{Rn}{Rr + Rn} \quad \text{EQ. 5}$$

POD describes the ability of the model to identify precipitation areas and FAR describes the erroneously detected precipitation areas. A perfect system has $POD = 1$ and $FAR = 0$.

The validation analysis in this report is performed manually using collocated satellite and synoptic observations presented in the graphical software DFELT[1]. When a pixel was to be classed as *Sn*, *Sr*, *Rn*, or *Rr* the box defined in FIGURE 5 was searched for each synoptic observation. If the box contained at least one pixel where the precipitation class were the same as the observation it was treated as correct. E.g. if the synoptic observation shows no precipitation at the station, and the 11×11 box contains pixels mainly classed as precipitation, except for a few that are classed as no precipitation, then this pixel is put in *Sn* category above. This is done to account for the potential time difference between the satellite observation and the synoptic observation.

The synoptic code for present weather is used for comparison of the analysed amount of precipitation. This reports precipitation as slight, moderate or heavy as well as indicating whether it is showers or not. Thus, more information can be read from the illustrations of combined satellite and synoptic observations than from the more objective validation. No thorough analysis of this is made in the report as the data material is too sparse.

## 4.4 Results

Eight days of satellite imagery close to 12:00 UTC was analysed in the period 6-13 August 1998. Validation results for all observations are presented in TABLE V. The individual results are presented as images with the synoptic observations overlaid. Interpretation of the colour codes used is given in FIGURE 6. Synoptic observations are plotted with codes for total cloud cover, and low, medium and high level clouds are plotted along with the present weather. For interpretation of the symbols[2] it is referred to e.g. Appendix E in Neiburger, Edinger and Bonner (1982).

The validation analysis was performed for each satellite scene, but as the number of synoptic observations in each scene is very low results are only presented for the whole period and not for each individual scene.

TABLE V shows that the ability of the model to identify precipitation areas is 0.7 and that its false alarm rate is 0.4. These results are promising given that no tuning of the model for this specific case was performed.

**TABLE V Validation results for the precipitation analysis during the whole period.**

| Variable | Count | Result |
|---|---|---|
| *Sn* | 98 | $POD = 0.7$ |
| *Sr* | 8 | |

1. Graphical presentation software for meteorological data developed at DNMI.
2. Standards are given by World Meteorological Organization.

**TABLE V Validation results for the precipitation analysis during the whole period.**

| Variable | Count | Result |
|---|---|---|
| *Rn* | 17 | *FAR* = 0.4 |
| *Rr* | 22 | |

While TABLE V presented the overall performance of the method during one week in August 1998, the performance of the method on each satellite scene analysed is briefly described in the remaining of this chapter. The colour table explanation given in FIGURE 6 describes the classes used here. If clouds are not classified as precipitating, they are classified according to the height of their cloud tops.


**FIGURE 6** *Colour explanation for the precipitation analysis imagery presented.*

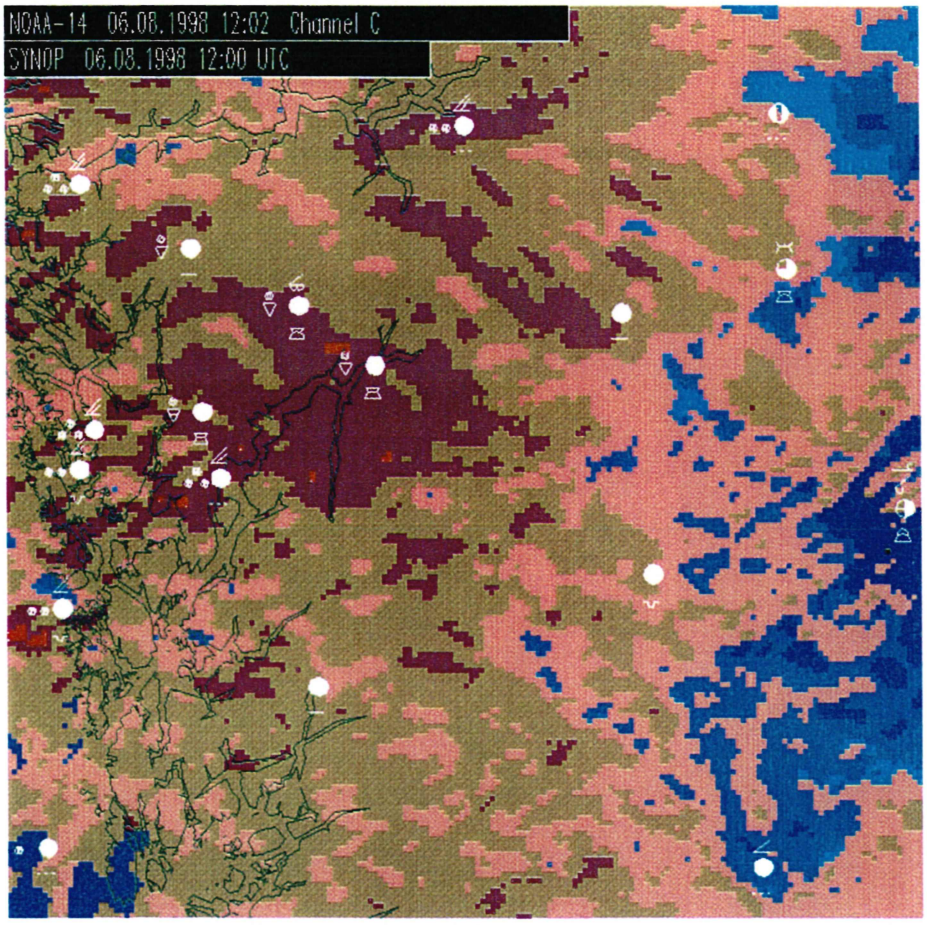


**FIGURE 7**

*Precipitation analysis performed on data collected from NOAA-14 on 6 August 1998, 12:02 UTC. The analysis is performed using HIRLAM data from 00:00 UTC model run valid for 12:00 UTC. Synoptic observations collected at 12:00 UTC are overlaid.*

The precipitation analysis for 6 August is presented in FIGURE 7 following the colours in FIGURE 6. This situation shows quite good resemblance between the synoptically observed precipitation and the precipitation analysis. Quite large areas are classed with risk of precipitation and slight precipitation, but also moderate and heavy precipitation is indicated in the analysed imagery. It is difficult to validate the qualitative assessment of the precipitation intensity due to the sparse observation network and complex topography of Norway. However, at least on the western part of the test area there seems to be some relevance in the qualitative precipitation intensity estimates. Here observed moderate precipitation areas compare well with the moderate and heavy precipitation areas in the precipitation analysis. It might be that precipitation areas are overestimated in the eastern part of the area, but once again the complex topography complicates this validation.

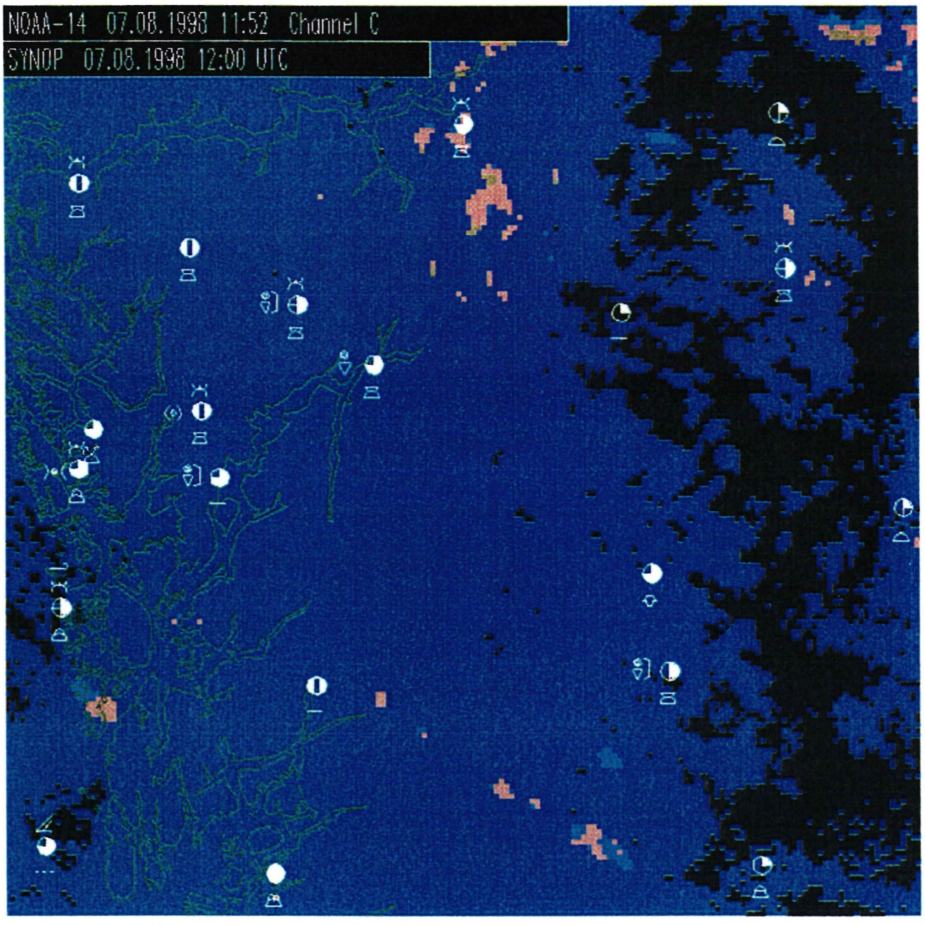


**FIGURE 8**

*Precipitation analysis performed on data collected from NOAA-14 on 7 August 1998, 11:52 UTC. The analysis is performed using HIRLAM data from 06:00 UTC model run valid for 12:00 UTC. Synoptic observations collected at 12:00 UTC are overlaid.*

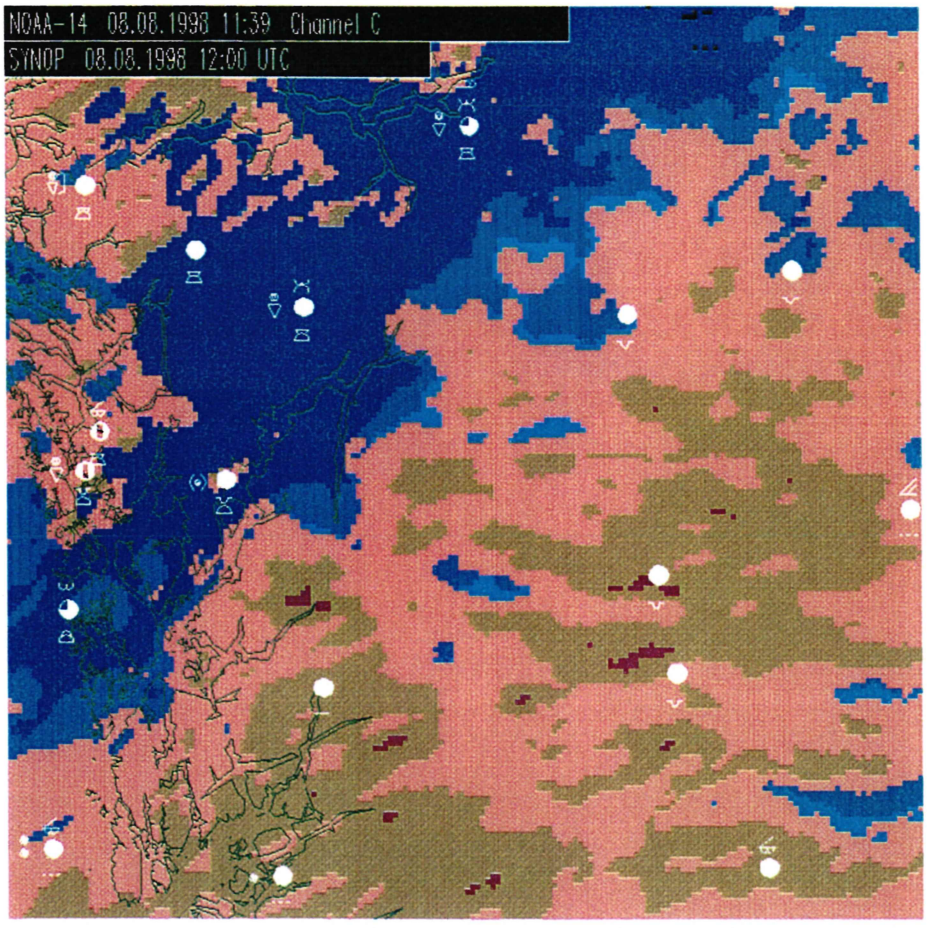


FIGURE 9

*Precipitation analysis performed on data collected from NOAA-14 on 8 August 1998, 11:39 UTC. The analysis is performed using HIRLAM data from 06:00 UTC model run valid for 12:00 UTC. Synoptic observations collected at 12:00 UTC are overlaid.*

The precipitation analysis of 7 August is presented in FIGURE 8. Precipitation was observed at some stations in Hordaland and Rogaland and at a single station in Telemark. Some of these observations indicate showers and not continuous precipitation. Very few pixels were classed as precipitation by the analysis scheme. The spatial distribution of pixels classified as precipitation in the satellite scene indicates that showers are present. As the nature of precipitation this day had a tendency towards showers, the analysis is good as scattered pixels with precipitation is found.

FIGURE 9 shows the precipitation analysis of 8 August. Large areas are classified with risk of precipitation. In the western part of Norway this seems to compare well with observations, but in the eastern part no precipitation was observed though large areas are classed as precipitating and even moderate in some smaller areas. The general impression is that convective clouds dominate in west and stratus clouds in the east. In Hordaland and Sogn og Fjordane some observed precipitation was not detected by the analysis scheme. The mis-classified precipitation pixels seems to be caused by low level Stratocumulus and medium level Altostratus. Both these cloud types are known to give risk of precipitation.

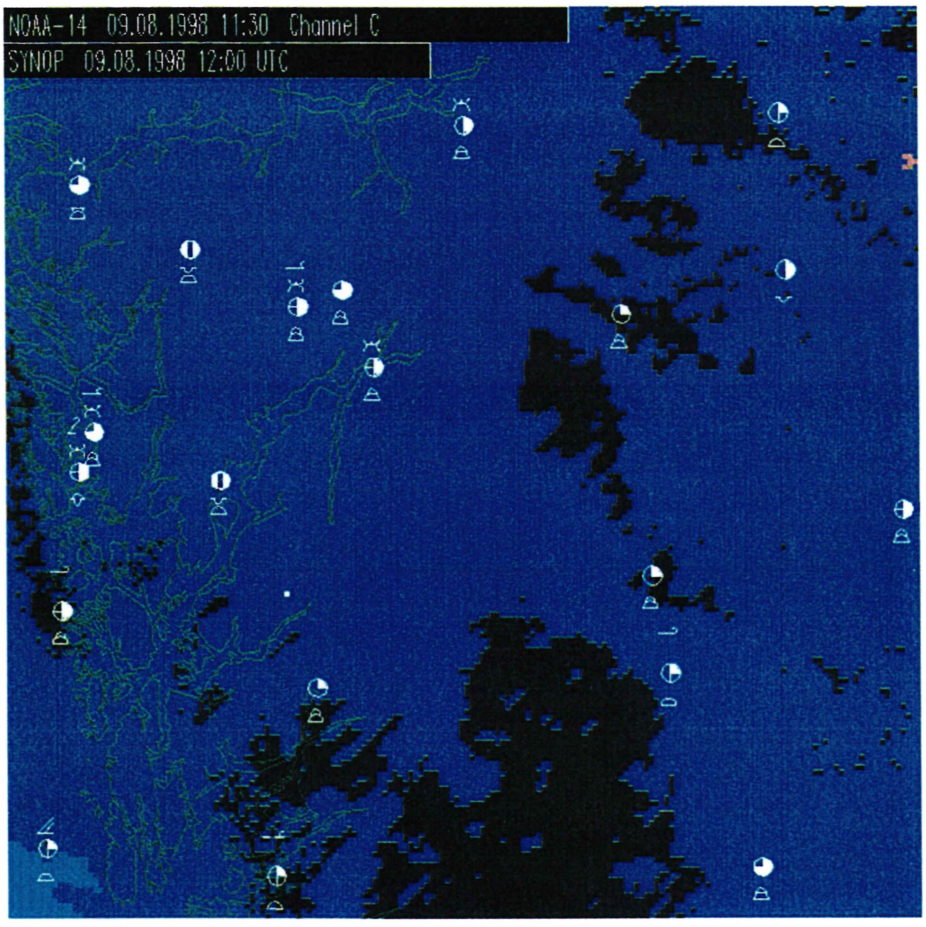


**FIGURE 10**

*Precipitation analysis performed on data collected from NOAA-14 on 9 August 1998, 11:30 UTC. The analysis is performed using HIRLAM data from the 00:00 UTC model run valid for 12:00 UTC. Synoptic observations collected at 12:00 UTC are overlaid.*

On 9 August (FIGURE 10), precipitation was not observed anywhere in the area. However, some pixels in the eastern (right) part of the area, far from the nearest synoptic station was classified as precipitation.

The precipitation analysis of 10 August is presented in FIGURE 11. No precipitation was observed. Some pixels in the southern part (lower) of the imagery was classified as risk of precipitation. Given the synoptic observations here this seems to be erroneous. High level clouds are overlaying low and medium level clouds. This might be the cause of the misinterpretation as spectral signatures are altered by this layering. An extensive cover of Cirrostratus overlaying Altocumulus are in this case misinterpreted.

On 11 August (FIGURE 12), no observations show precipitation. An area close to Hardangerfjord in western Norway (left part of area) is classified as precipitating. This area compares well with the glacier Folgefonn. It may be that the glacier is misinterpreted as precipitation, but it might as well be that it actually is precipitating at the glacier. No synoptic observations are available to determine this. Further north (upwards), the glacier Hardangerjøkulen was identified as snow/ice, two pixels in this area are identified as risk of precipitation. The synoptic observations indicate presence of thin Cirrus or thin Altocumulus.

On 12 August (FIGURE 13), precipitation is observed in western Norway (left part of area) close to Bergen. The precipitation analysis identifies areas of precipitation in almost the whole area analysed. Synoptic cloud observations indicate convective activity at low level (towering Cumulus) and areas of Altostratus.

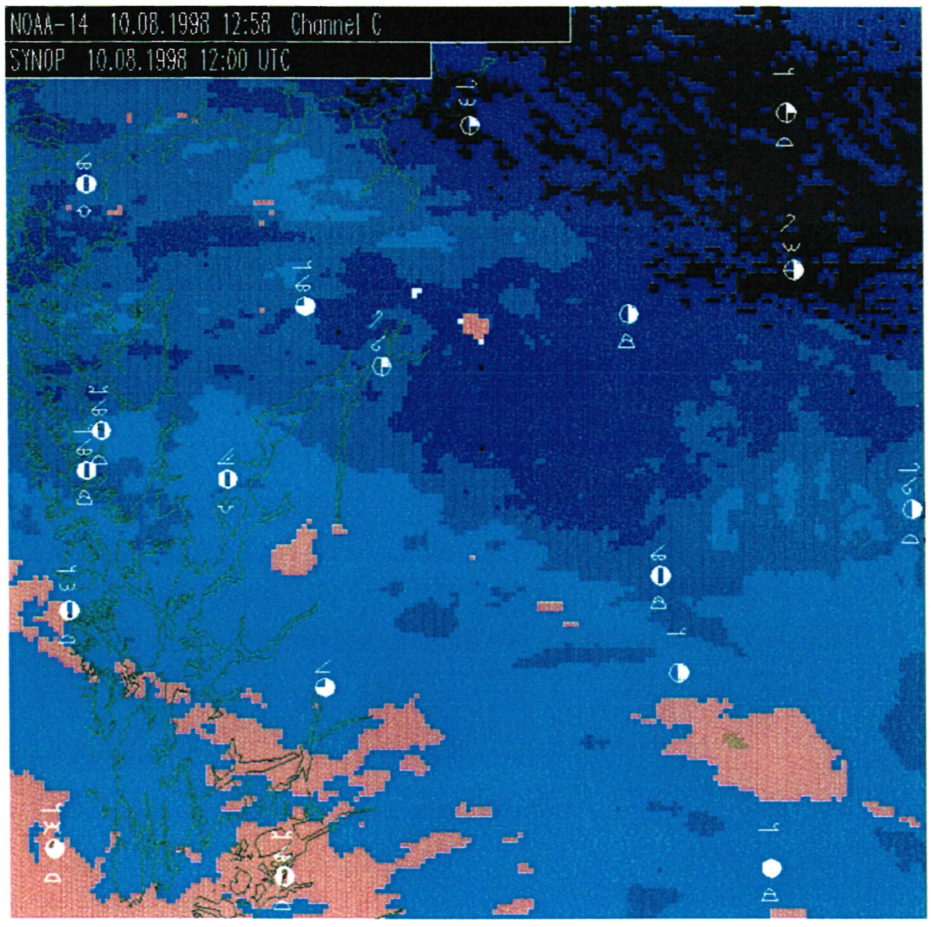


**FIGURE 11**

*Precipitation analysis performed on data collected from NOAA-14 on 10 August 1998, 12:58 UTC. The analysis is performed using HIRLAM data from the 00:00 UTC model run valid for 12:00 UTC. Synoptic observations collected at 12:00 UTC are overlaid.*

The precipitation analysis of 13 August is presented in FIGURE 14. Precipitation is observed in the middle part of the area. The precipitation analysis identifies precipitation in most of the area, especially in the eastern (right) part. Synoptic cloud observations in the southern part (lower) show Altostratus overlaying low level stratus clouds, some places precipitating and some places not. Further north, close to Hardangerfjord and Sognefjord, precipitation is observed in connection with convective clouds. In the eastern part of the area, precipitation is observed from low level clouds.

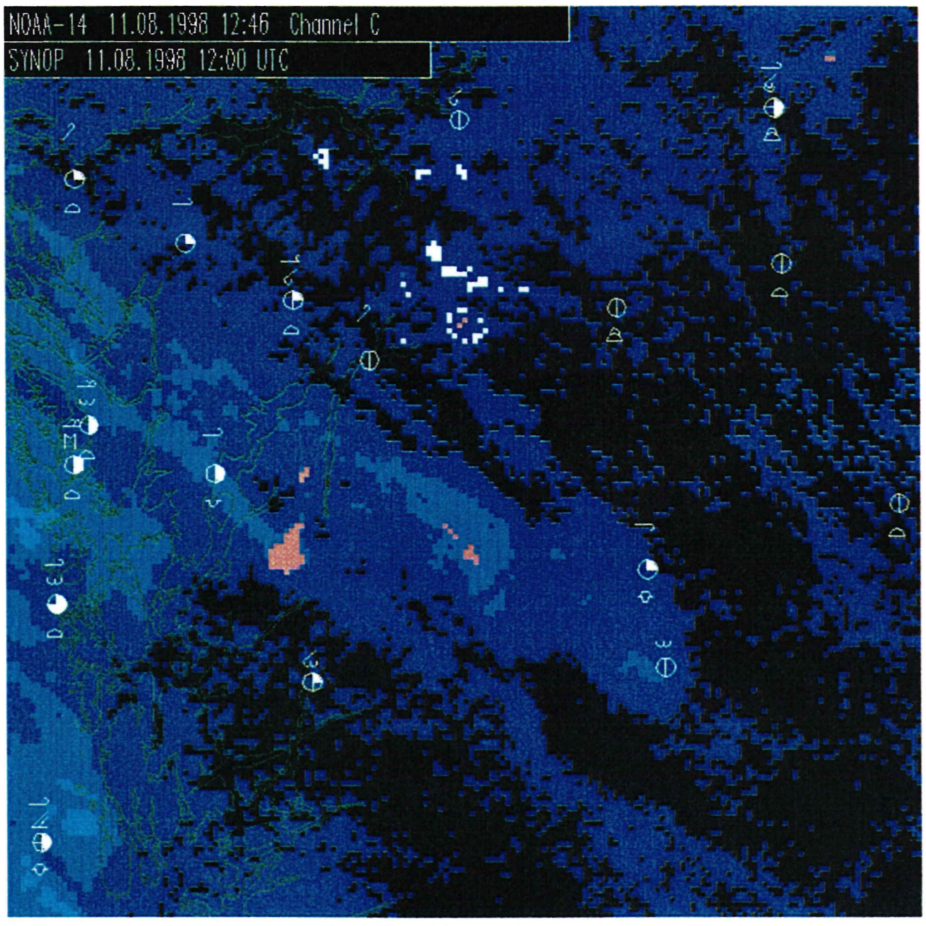


**FIGURE 12**

*Precipitation analysis performed on data collected from NOAA-14 on 11 August 1998, 12:46 UTC. The analysis is performed using HIRLAM data from the 06:00 UTC model run valid for 12:00 UTC. Synoptic observations collected at 12:00 UTC are overlaid.*

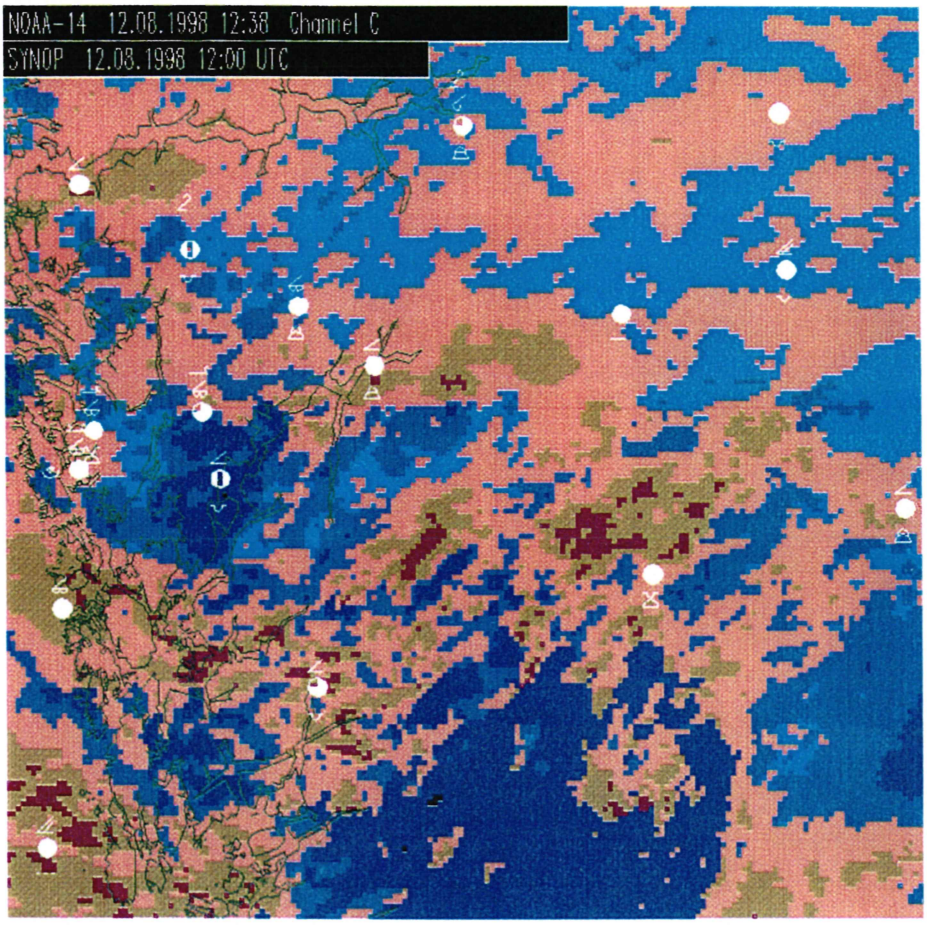


**FIGURE 13**

*Precipitation analysis performed on data collected from NOAA-14 on 12 August 1998, 12:38 UTC. The analysis is performed using HIRLAM data from the 00:00 UTC model run valid for 12:00 UTC. Synoptic observations collected at 12:00 UTC are overlaid.*

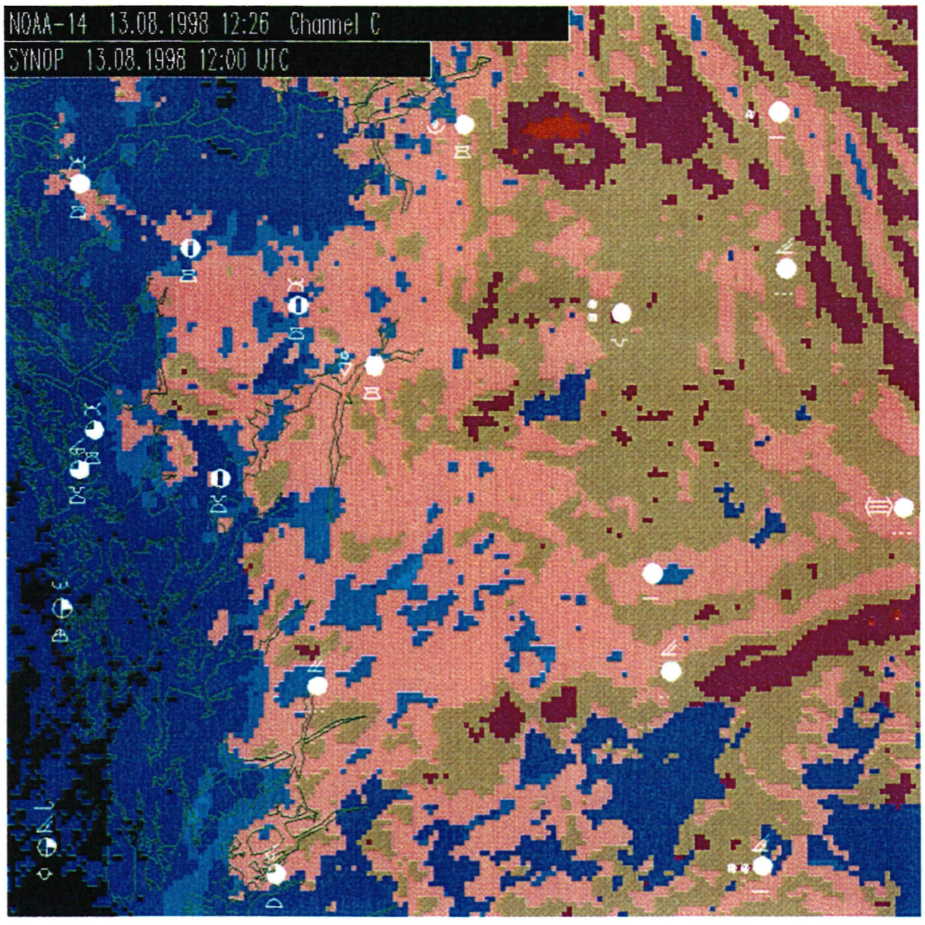


**FIGURE 14**

*Precipitation analysis performed on data collected from NOAA-14 on 13 August 1998, 12:26 UTC. The analysis is performed using HIRLAM data from the 06:00 UTC model run valid for 12:00 UTC. Synoptic observations collected at 12:00 UTC are overlaid.*

## 4.5 Discussion

Problems in the classification seems to be connected to Altostratus and Stratocumulus. Both these cloud types are known to give possibilities for precipitation. Tuning of the algorithms may improve the *POD* and *FAR* in these circumstances. However, as the difference in spectral signature between the precipitating and non-precipitating versions of these clouds is small, more benefit would probably be gained by using SSM/I data as an additional data source.

Another potential source of errors is thin clouds overlaying snow or ice surfaces. The present use of the T4-T5 feature is not well tuned. Improvements are expected when 10-bits data with satellite zenith angle is used. However, thin clouds overlaying snow or ice may alter the spectral signature in this feature and will probably contribute to the *FAR* ratio anyway.

In order to improve this system a validation programme utilizing other parameters than the subjective synoptic parameters is required. As these are not good validation parameters.

CHAPTER 5

# Summary

A prototype of a precipitation analysis scheme using AVHRR data is developed at DNMI. Preliminary results shows that this has good potential for detecting precipitation areas, however at present the probability score is too low and the false alarm rate too high. Tuning of the system is required, as well as an improved validation program.

The system is able to give a qualitative indication of the spatial variability of precipitation. In order to gain a quantitative measure, additional data sources like SSM/I and/or weather radar has to be used.

The main problem using AVHRR data for precipitation analysis is that this instrument do not observe precipitation directly, but cloud properties which indirectly may be related to precipitation. SSM/I data are very useful over ocean, but are harder to use over land surfaces and the footprint of this instrument is large compared to AVHRR and weather radar. However, the use of these data in addition to AVHRR should be tested. The most promising additional data source is the weather radar. At present the data coverage is limited to Southeast Norway, but will be extended further west by a new radar during the summer of 1999. Further development of the radar network is defined as a main priority for DNMI.

A large potential for improved precipitation estimates lies in the combined use of several remote sensing techniques along with NWP models.

# References

Arkin, P.A, 1984: An examination of the Southern Oscillation in the upper tropospheric tropical and subtropical windfield, *Ph.D. dissertation, University of Maryland*, 240 pp.

Arkin, P.A., and B. Meisner, 1987: The relationship between large-scale convective rainfall and cold over the Westerne Hemisphere during 1982-1984, *Mon. Wea. Rev.*, **Vol. 115**, pp. 51-74.

Bellon, A., A. Kilambi, G.L. Austin, and M.R. Duncan, 1992: A satellite and radar rainfall observational and forecasting system, *Preprint Vol., AMS 6th Conf. Satellite Meteorology and Oceanography*, Atlanta.

Bellon, A., S. Lovejoy, and G.L. Austin, 1980: Combining satellite and radar data for the short-range forecasting of precipitation, *Mon. Wea. Rev.*, **Vol. 108**, pp. 1554-1556.

Breivik, L.-A., S. Eastwood, Ø. Godøy, J. Sunde, C. Ulstad, 1997: Satellite derived Sea Ice and Sea Surface Temperatures (SST) at DNMI Status Report from March 1997, *DNMI Res. Note*, No. 4, Norwegian Meteorological Institute, Norway, ISSN 0332-9879, 35 pp.

Eastwood, S., 1996: Nedbør over Norden avledet fra AVHRR data, *Hovedoppgave i Meteorologi (Master thesis), Institutt for Geofysikk, University of Oslo, Norway*, (In norwegian).

Follandsbee, W.A., 1973: Estimation of average daily rainfall from satellite cloud photographs, *NOAA Technical Memorandum NESS 44*, Dept. of Commerce, Washington, DC, 39 pp.

Godøy, Ø., 1998: The SAGOB database, *Internal DNMI MEMO*, Norwegian Meteorological Institute, Norway, 5 pp.

Godøy, Ø., 1997: Cloud masking using AVHRR/2, current status in the objective analysis system, *DNMI Res. Note*, No. 7, Norwegian Meteorological Institute, Norway, ISSN 0332-9879, 15 pp.

Godøy, Ø., and J. Sunde, 1996: Processing and objective classification of AVHRR data at DNMI, *DNMI Res. Rep.*, No. 39, Norwegian Meteorological Institute, Norway, ISSN 0332-9879, 71 pp.

Griffith, C.G., W.L. Woodley, P.G. Grube, D.W. Martin, J. Stout, and D.N. Sikdar, 1978: Rain estimation from geosynchronous satellite imagery-visible and infrared studies, *Mon. Wea. Rev.*, **Vol. 106**, pp. 1153-1171.

Inoue, T., 1987: An Instantaneous Delineation of Convective Rainfall Areas Using Split Window Data of NOAA-7 AVHRR, *J. Met. Soc. Jap.*, **Vol. 65**, No. 3, pp. 469-480.

Jackson, P., G.E. Holpin, J.S. Foot, and R. Allam, 1995: The detection of mid-latitude precipitation from AVHRR and SSM/I: Results from a comparison of algorithms, *Proc. 1995 Met. sat. data users' conf.*, EUMETSAT, pp. 401-408.

Karlsson, K.-G., 1997: An introduction to Remote Sensing in Meteorology, Swedish Meteorological and Hydrological Institute, ISBN 91-87996-08-1.

Karlsson, K.-G., 1993: Comparison of operational AVHRR-based cloud analyses with surface observations, *Proc. 6$^{th}$ European AVHRR Data User's Meeting*, EUMETSAT, EUM P12, pp. 223-230.

Kidder, S.Q. and T.H. Vonder Haar, 1995: Satellite Meteorology, Academic Press, ISBN 0-12-406430-2.

Liljas, E., 1986: Use of the AVHRR 3.7 micrometer channel in multispectral cloud classification, *SMHI Promis-Rapporter*, 1986, Nr. 2.

Lovejoy, S., and G.L. Austin, 1979: The delineation of rain areas from visible and infrared data for GATE, and mid-latitudes, *Atm.-Ocean*, **Vol. 17**, pp. 77-92.

Negri, A.J., R.F. Adler, and P.J. Wetzel, 1984: Rain estimation from satellites: An examination of the Griffith-Woodley technique, *J. Appl. Meteor.*, **Vol. 32**, pp. 102-116.

Neiburger, M., J.G. Edinger, and W.D. Bonner, 1982: Understanding our atmospheric environment, W.H. Freeman and Company, ISBN 0-7167-1348-9.

Petty, G.W., 1995: The Status of Satellite-Based Rainfall Estimation over Land, *Rem. Sens. Env.*, **Vol. 51**, pp. 125-137.

Petty, G.W., 1990: On the response of the Special Sensor Microwave Imager to the marine environment - Implications for atmospheric parameter retrievals, *Ph. D. dissertation, Technical Report NASA Grant NAG5-943*, 292 pp.

Setvak, M., and C.A. Doswell III, 1991: The AVHRR Channel 3 Cloud Top Reflectivity of Convective Storms, *Mon. Wea. Rev.*, **Vol. 119**, pp. 841-847.

Scofield, R.A., 1987: The NESDIS operational convective precipitation technique, *Mon. Wea. rev.*, **Vol. 115**, pp. 1773-1792.

Spencer, R.W., H.M. Goodman and R.E. Hood, 1989: Precipitation retrieval over land and ocean with the SSM/I: Identification and characteristics of the scattering signal, *J. Atmos. Ocean. Tech.*, **Vol. 6**, pp. 254-273.

Tipler, P.A., 1982: Physics, Worth Publishers Inc., ISBN 0-87901-135-1.

Wu, R., J.A. Weinman, and R.T. Chin, 1985: Determination of rainfall rates from from GOES satellite images by a pattern recognition technique, *J. Atm. Ocean Tech*, **Vol. 2**, pp. 314-330.

# UTGITTE NOTAT I HYDRA-SERIEN

1/97 **Metoder for kvantifisering av hydrologiske prognosefelts representativitet.**
Kai Fjelstad, NLH (diplomarbeid).

2/97 **Effekter av flomsikringstiltak. En gjennomgang av litteraturen.**
Magne Wathne, SINTEF.

3/97 **Virkningen av lokal overvannsdisponering på tettstedsflommer.**
Dag Rogstad og Bjørn Vestheim, NLH (hovedoppgave).

4/97 **Forslag til kravspesifikasjon av vassdragsmodell.**
Lars A. Roald, NVE.

5/97 **A note on floods in high lattitude countries.**
Lars A. Roald, NVE.

6/97 **Climate change and floods.**
Nils Roar Sælthun, NIVA.

7/97 **Flomdemping i Gudbrandsdalslågen. Programstruktur og systembeskrivelse.**
Magne Wathne og Knut Alfredsen, SINTEF.

8/97 **Klima, arealbruk og flommer i perspektiv.**
Arnor Njøs, Jordforsk.

9/97 **Flood forecasting in practice.**
Dan Lundquist, GLB.

1/98 **Bruk av ensembleprognoser til estimering av usikkerhet i lokale nedbørprognoser.**
Marit Helene Jensen, DNMI.

2/98 **LANDSKAP OG ESTETIKK –et kulturelt perspektiv.**
Oddrun Sæter, Byggforsk.

3/98 **Betydning av vårflommens størrelse for tetthet av laks- og ørretunger i Saltdalselva.**
Arne J. Jensen og Bjørn Ove Johnsen, NINA.

4/98 **Pure Model Error of the HBV-model.**
Øyvind Langsrud, Arnoldo Frigessi and Gudmund Høst, Norwegian Computing Center
(Norsk Regnesentral)

5/98 **Analyse av effekter av urbanisering og avrenningsutjevnende tiltak i Svebestadfeltet – Sandnes kommune.**
Jadranka Milina, SINTEF.

6/98 **Virkning av urbanisering på avrenningsforhold i Storånavassdraget.**
Jadranka Milina, SINTEF.

7/98 **Metodebeskrivelse for flomsoneanalyse med eksempler fra Flisa og Kirkenær.**
Søren Elkjær Kristensen og Astrid Voksø, NVE.

8/98 **Statistical Forecasting of Precipitation Conditional on Numerical Weather Prediction Models.**
John Bjørnar Bremnes, DNMI

9/98 **1995-flommens volum, stigningstid og varighet i Gudbrandsdalslågen.**
Jan Ove Søderholm (Hovedfagsoppgave ved Geografisk Institutt, Universitetet i Oslo, våren 1998).

10/98 **Vårflommer i Glomma. Modellering av maksimalvannføringen på bakgrunn av volum og flomhydrogrammets form.**
Grete Orderud Solberg (Hovedfagsoppgave ved Geografisk Institutt, Universitetet i Oslo, våren 1998).

11/98 **Flomvolum Østlandet våren 1995. Frekvens og regional fordeling.**
Grete Orderud Solberg og Kjell Nordseth. Geografisk Institutt, Universitetet i Oslo.

12/98 **A Statistical Model for the Uncertainty in Meteorological Forecasts, with Applications to the Knappom and Røykenes Catchments.**
Turid Follestad og Gudmund Høst. Norwegian Computing Center (Norsk Regnesentral)

13/98 **Precipitation estimation using satellite remote sensing.**
Øystein Godøy, Det norske meteorologiske institutt.


# Kontaktpersoner

***formann i styringsgruppen:*** Ola Skauge
Tlf. 73 58 05 00
E-post: ola.skauge@dirnat.no

***programleder:*** Arnor Njøs
Jordforsk
Tlf. 64 94 81 70 (Jordforsk)
Tlf. 22 95 90 98 (NVE)
E-post: arnor.njos@jordforsk.nlh.no
E-post: xarn@nve.no.

***naturgrunnlag og arealbruk:*** Arne Grønlund
Jordforsk
Tlf. 64 94 81 09
E-post: arne.gronlund@jordforsk.nlh.no

Noralf Rye
Universitetet i Bergen
Tlf. 55 58 34 98
E-post: noralf.rye@geol.uib.no

***tettsteder:*** Oddvar Lindholm
Norges Landbrukshøgskole
Tlf. 64 94 87 08
E-post: oddvar.lindholm@itf.nlh.no

***flomdemping, flomvern og flomhandtering:*** Dan Lundquist
Glommens og Laagens Brukseierforening
Tlf. 22 54 96 00
E-post: danlund@sn.no

***skaderisikoanalyse:*** Nils Roar Sælthun
Norsk institutt for vannforskning
Tlf. 22 18 51 21
E-post: nils.saelthun@niva.no

***miljøvirkninger av flom og flomforebyggende tiltak:*** Olianne Eikenæs
Norges vassdrags- og energiverk
Tlf. 22 95 92 24
E-post: oli@nve.no

***databaser og GIS:*** Lars Andreas Roald
Norges vassdrags- og energiverk
Tlf. 22 95 92 40
E-post: lars.roald@nve.no

***modellarbeid:*** Ånund Killingtveit
Norges teknisk-naturvitenskaplige universitet
Tlf. 73 59 47 47
E-post: aanund.killingtveit@bygg.ntnu.no

***programadministrasjon:*** Olianne Eikenæs
Norges vassdrags- og energiverk
Tlf. 22 95 92 24
E-post: oli@nve.no
Hjemmeside: http://www.nve.no

Per Einar Faugli
Norges vassdrags- og energiverk
Tlf. 22 95 90 85
E-post: pef@nve.no